

Intra-colonial diversity in the scleractinian coral, *Acropora millepora*: identifying the nutritional gradients underlying physiological integration and compartmentalised functioning

Jessica A Conlan ^{Corresp., 1}, Craig A Humphrey ², Andrea Severati ², David S Francis ¹

¹ School of Life and Environmental Science, Deakin University, Warrnambool, Victoria, Australia

² The National Sea Simulator, Australian Institute of Marine Science, Townsville, Queensland, Australia

Corresponding Author: Jessica A Conlan

Email address: conlan@deakin.edu.au

Scleractinian corals are colonial organisms comprising multiple physiologically integrated polyps and branches. Colonialism in corals is highly beneficial, and allows a single colony to undergo several life processes at once through physiological integration and compartmentalised functioning. Elucidating differences in the biochemical composition of intra-colonial branch positions will provide valuable insight into the nutritional reserves underlying different regions in individual coral colonies. This will also ascertain prudent harvesting strategies of wild donor-colonies to generate coral stock with high survival and vigour prospects for reef-rehabilitation efforts and captive husbandry. This study examined the effects of colony branch position on the nutritional profile of two different colony sizes of the common scleractinian, *Acropora millepora*. For smaller colonies, branches were sampled at three locations: the colony centre (S-centre), 50% of the longitudinal radius length (LRL) (S-50), and the colony edge (S-edge). For larger colonies, four locations were sampled: the colony centre (L-centre), 33.3% of the LRL (L-33), 66.6% of the LRL (L-66), and the edge (L-edge). Results demonstrate significant branch position effects, with the edge regions containing higher protein, likely due to increased tissue synthesis and calcification. Meanwhile, storage lipid and total fatty acid concentrations were lower at the edges, possibly reflecting catabolism of high-energy nutrients to support proliferating cells. Results also showed a significant effect of colony size in the two classes examined. While the major protein and structural lipid sink was exhibited at the edge for both sizes, the major sink for high-energy lipids and fatty acids appeared to be the L-66 position of the larger colonies and the S-centre and S-50 positions for the smaller colonies. These results confirm that the scleractinian coral colony is not nutritionally homogeneous, and while different regions of the coral colony are functionally specialised, so too are their nutritional profiles geared toward meeting specific energetic demands.

1 Intra-colonial diversity in the scleractinian coral, *Acropora*
2 *millepora*: identifying the nutritional gradients underlying
3 physiological integration and compartmentalised functioning

4

5 Conlan, J A.^{1,2,*}, Humphrey, C.A.², Severati, A.², and D.S. Francis¹

6

7 ¹Deakin University, Geelong, Australia. School of Life and Environmental Sciences,
 8 Warrnambool Campus. Princes Hwy, Sherwood Park. PO Box 423, Warrnambool, VIC 3280

9 ²The National Sea Simulator; Australian Institute of Marine Science, PMB No3, Townsville,
 10 QLD 4810, Australia.

11 *Corresponding author (jessconlan@live.com.au)

13 Abstract

14 Scleractinian corals are colonial organisms comprising multiple physiologically integrated
 15 polyps and branches. Colonialism in corals is highly beneficial, and allows a single colony to
 16 undergo several life processes at once through physiological integration and compartmentalised
 17 functioning. Elucidating differences in the biochemical composition of intra-colonial branch
 18 positions will provide valuable insight into the nutritional reserves underlying different regions
 19 in individual coral colonies. This will also ascertain prudent harvesting strategies of wild donor-
 20 colonies to generate coral stock with high survival and vigour prospects for reef-rehabilitation
 21 efforts and captive husbandry. This study examined the effects of colony branch position on the
 22 nutritional profile of two different colony sizes of the common scleractinian, *Acropora*
 23 *millepora*. For smaller colonies, branches were sampled at three locations: the colony centre (S-
 24 centre), 50% of the longitudinal radius length (LRL) (S-50), and the colony edge (S-edge). For
 25 larger colonies, four locations were sampled: the colony centre (L-centre), 33.3% of the LRL (L-
 26 33), 66.6% of the LRL (L-66), and the edge (L-edge). Results demonstrate significant branch
 27 position effects, with the edge regions containing higher protein, likely due to increased tissue
 28 synthesis and calcification. Meanwhile, storage lipid and total fatty acid concentrations were
 29 lower at the edges, possibly reflecting catabolism of high-energy nutrients to support
 30 proliferating cells. Results also showed a significant effect of colony size in the two classes
 31 examined. While the major protein and structural lipid sink was exhibited at the edge for both
 32 sizes, the major sink for high-energy lipids and fatty acids appeared to be the L-66 position of the
 33 larger colonies and the S-centre and S-50 positions for the smaller colonies. These results
 34 confirm that the scleractinian coral colony is not nutritionally homogeneous, and while different

35 regions of the coral colony are functionally specialised, so too are their nutritional profiles
 36 geared toward meeting specific energetic demands.

37 **Introduction**

38 Scleractinian corals are colonial organisms comprising multiple asexually produced and
 39 physiologically integrated polyps (Mackie, 1986; Gateno et al., 1998). The colonial nature of
 40 scleractinian corals is highly beneficial, with modular coral colonies being able to attain large
 41 increases in size and volume isometrically, allowing the component units to remain small
 42 (Vollmer & Edmunds, 2000; Hughes, 2005). This greatly reduces the chance of whole colony
 43 mortality and increases colony exposure to exploitable environmental factors, such as sunlight
 44 and sources of nutrition (Nakamura & Yamasaki, 2006; Bone & Keough, 2010).

45 Physiological integration also permits colony-wide resource translocation from branches
 46 growing in favourable microhabitats to those growing under more adverse conditions (Hemond,
 47 Kaluziak & Vollmer, 2014; Nozawa & Lin, 2014). This is made possible through interconnecting
 48 tissue between polyps and a shared gastrovascular circulatory system (Hemond, Kaluziak &
 49 Vollmer, 2014). Individual polyps can thus act as cooperative systems, buffering the negative
 50 microhabitat effects, colonising hostile areas, supplying colony areas that do not possess feeding
 51 polyps, and permitting resource sharing should some polyps fail to capture food or light (Gateno
 52 et al., 1998).

53 Additionally, intracolony transport of materials and metabolites via the gastrovascular system
 54 provides a means of transferring essential resources from established regions and concentrating
 55 them in zones of maximal energetic demand (Taylor, 1977). For example, organic products
 56 (largely lipids, glycerol, and glucose) have been shown to be translocated from the established
 57 branch bases to the growing tips, in order to contribute to calcification and tissue synthesis
 58 (Fang, Chen & Chen, 1989; Oren, Rinkevich & Loya, 1997). Established colony areas such as
 59 lower branch regions face less competitive interactions and are no longer undergoing rapid

growth, and thus possess higher energy reserves (Oku et al., 2002). Meanwhile, growing regions with proliferating cells have higher metabolic rates and thus greater energetic demand (Gladfelter, Michel & Sanfelici, 1989; Oku et al., 2002).

Different colony regions can also be specialised for specific functions. For example, established colony regions are generally the most fecund, while the growing regions are often sexually sterile, and dedicated to growth and asexual reproduction (Nozawa & Lin, 2014). Such compartmentalisation of functional roles transcends to physiological processes. It is therefore reasonable to hypothesise that this, in turn, should manifest in zonation of nutritional resources and bioactive compounds, since different nutrients are required to fuel different life processes (Sargent et al., 1999b). For example, the quantity and nature of coral lipids and their constituent fatty acids (FA) varies significantly with photosynthesis, respiration, heterotrophy, cell replenishment, and reproduction (Ward, 1995; Leuzinger, Anthony & Willis, 2003; Imbs, 2013). In particular, high photosynthesis rates can be characterised by an abundance of carbon-rich compounds (Muscatine, 1990), while heterotrophically-derived nutrients are richer in nitrogen and phosphorus (Houlbrèque & Ferrier-Pagès, 2009). Additionally, protein fuels tissue growth, organogenesis, and calcification (Ramos-Silva et al., 2014), as well as high metabolic rates in corals (Gladfelter, Michel & Sanfelici, 1989; Oku et al., 2002).

While numerous studies have reported on intra-colonial variation in the biochemical composition along a single coral branch (i.e. branch base-tip) (Taylor, 1977; Fang, Chen & Chen, 1989; Gladfelter, Michel & Sanfelici, 1989; Oku et al., 2002; Tang et al., 2015), these results provide little insight into nutritional processes within the colony as a whole. To date, a comprehensive analysis extrapolating these findings to nutritional variation between colony regions (i.e. colony centre to edge) has yet to be conducted. Identifying the presence of nutritional

compartmentalisation in coral colonies *in toto* would augment current understanding of colonial integration and the nutritional resources driving functional roles in healthy coral today, which is fundamental in informing coral reef research and management practices in the future.

Elucidating intracolony variation in the nutritional profile may also facilitate an improved harvesting strategy of wild donor coral colonies, permitting judicious selection of branches with maximal survival, growth, and vigour prospects following fragmentation and translocation for reef rehabilitation efforts and captive husbandry (Olivotto et al., 2011; Leal et al., 2016).

Increased global awareness of coral reef degradation has resulted in the development of rehabilitation strategies including fragmentation and translocation, to enable rapid regeneration of degraded reef sites (Forsman et al., 2015). However, fragmentation and translocation are highly stressful events for coral, and reports of successful cultivation from fragmented branches are sparse (Arvedlund, Craggs & Pecorelli, 2003; Leal et al., 2016).

Fragmentation causes tissue loss, lesions, and initial reduction in colony size, which leads to an extensive and vulnerable period of recovery and regeneration (Smith & Hughes, 1999; Lirman, 2000a). This is exacerbated by the translocation of coral fragments into foreign conditions, where water quality, temperature, light intensity, and feed availability can vary significantly from the environment of origin. Importantly, the size and quality of initial energy reserves have been shown to significantly influence coral survivorship following stressful events (Anthony et al., 2009; Sheridan et al., 2013). As such, identifying the colony branch locations that possess ‘optimal’ nutritional profiles would be advantageous to buffer the stressors associated with fragmentation and translocation.

In addition, the size of the coral colony has been shown to influence several aspects of a coral’s physiology, including energy allocation to growth (Anthony, Connolly & Willis, 2002),

reproduction (Nozawa & Lin, 2014), and primary production (Jokiel & Morrissey, 1986) - inferring that the nutritional drivers behind these processes should also vary among different colony size classes. As such, this study sought to test two hypotheses; 1) that coral branch biochemical composition will differ depending on its originating position within the colony, and 2) that the overall colony size will influence the regional trends in branch biochemical composition. Here, we examined the nutritional composition along the longitudinal radius of two different size classes of a common, broadcast spawning scleractinian coral, *Acropora millepora*.

Materials and Methods

Sample collection

Sampling was conducted at depths of 2.6 – 5.4 m at Davies Reef in the Great Barrier Reef, Queensland, Australia (lat.: -18° 49.948'S, long.:147° 37.995'E) on the 9th of June, 2015. Ten colonies of two size classes of *Acropora millepora* were sampled (Field collections were approved by the Great Barrier Reef Marine Park Authority: G12/35236.1). The two size classes were larger: $4376 \pm 741 \text{ cm}^2$, and smaller: $1410 \pm 88 \text{ cm}^2$ (planar surface area), which represented two common size classes in the sampling area. For each colony, two replicate, adjacent branches were sampled from each location. For smaller colonies, branches were sampled at three locations: the centre of the colony (S-centre), 50 % of the longitudinal radius length (S-50), and the edge of the colony (S-edge) (Fig. 1). For larger colonies, four locations were sampled: the centre of the colony (L-centre), 33.3 % of the longitudinal radius length (L-33), 66.6 % of the longitudinal radius length (L-66), and at the edge (L-edge).

Zooxanthellae densities

Zooxanthellae were extracted using the air-spraying technique (Szmant & Gassman, 1990). A 500 uL aliquot of tissue slurry was taken and combined with a 500 uL aliquot of 3 % formalin: filtered seawater for preservation. Zooxanthellae were counted in triplicate using a haemocytometer. Zooxanthellae densities were then standardised to branch surface area (cm²), which was obtained through the simple geometry technique, which has been shown to be suitable for *Acropora* spp. (Naumann et al., 2009), using the software, Fiji ImageJ (Schindelin et al., 2012). Due to the presence of large quantities of organic material in coral skeletons (Conlan, Rocker & Francis, 2017), once the zooxanthellae aliquot was taken, the denuded skeletons were crushed and recombined with the sprayed tissue for further analyses.

Proximate analysis

Once the zooxanthellae aliquot was taken, the tissue slurry and denuded skeletons were freeze-dried for 72 hrs. Skeletons were then crushed using a mortar and pestle under a French press and the resultant powder was recombined with the dried tissue. The recombined coral powder was then extracted for total lipid content according to the method described in Conlan *et al.* (2014). Dry samples were weighed then soaked overnight in a 3 mL aliquot of dichloromethane: methanol (CH₂Cl₂:CH₃OH). The following morning, this mixture was filtered and the solid residue re-suspended and soaked for a further 10 min with another 3 mL aliquot of CH₂Cl₂:CH₃OH, followed by a further filtration step. This process was repeated three times. The combined filtrates (~9 mL) were then transferred into a separation funnel and combined with a

4.5 mL sample washing solution of KCl (0.44 %) in H₂O/CH₃OH (3:1). The mixture was shaken vigorously and allowed to settle overnight. The following morning, the bottom layer containing the extracted lipid was recovered and the solvent was evaporated under nitrogen. The lipid content was then quantified the four decimal places . Protein content was determined according to the Kjeldahl method (crude protein calculated as nitrogen \times 6.25) in an automated Kjeltech (Tecator, Sweden). Total ash was determined by incineration in a muffle furnace (C & L Fetlow, Model WIT, Blackburn, Victoria, Australia) at 450 °C for 12 h. The ash content was subtracted from the total composition to obtain ash free dry weight (AFDW), which excludes the inorganic component. Nitrogen free extract (NFE) was obtained by subtracting the ash, lipid, and protein from the total sample mass. Energy was calculated using the enthalpies of combustion for lipid (39.5 J mg⁻¹) and protein (23.9 J mg⁻¹) from Gnaiger & Bitterlich (1984).

Lipid class and fatty acid analysis

Lipid class analysis was determined using an Iatroscan MK 6s thin layer chromatography-flame ionisation detector (Mitsubishi Chemical Medience, Tokyo Japan) according to the method of Conlan et al (2014). Briefly, each sample was spotted in duplicate on silica gel S5-chromarods (5 µm particle size) with lipid separation following a two-step elution sequence: 1) elution of phosphatidylethanolamine (PE), phosphatidylcholine (PC) and lysophosphatidylcholine (LPC) was achieved in a dichloromethane/methanol/water (50:20:2, by volume) solvent system run to half height (~15 min); and 2) after air drying, elution of wax esters (WAX), triacylglycerol (TAG), free fatty acid (FFA), 1,2-diacylglycerol (1,2DAG) and sterol (ST) was achieved in a hexane/diethyl ether/formic acid (60:15:1.5, by volume) solvent system run to full height (~30

min). Since glycolipids commonly elute with monoacylglycerols and pigments, including chlorophyll, the term “acetone mobile polar lipid” (AMPL) was used in the present study (Parrish, Bodennec & Gentien, 1996). AMPL was quantified using the 1-monopalmitoyl glycerol standard (Sigma-Aldrich Co., USA), which has demonstrated a response that is intermediate between glycolipids and pigments (Parrish, Bodennec & Gentien, 1996).

Following initial lipid extraction, FA were esterified into methyl esters using an acid-catalysed methylation method and then analysed by gas chromatography as recently described in Conlan et al (2014).

Statistical analysis

Data were analysed statistically using R software version 2.3.1 (RStudio Team, 2015; R Development Core Team, 2016). Due to non-normality and heteroscedasticity (detected via Shapiro-Wilk and Levene’s tests, respectively), as well as some negative values, data were transformed using a Yeo-Johnson power transformation (*caret* package (Kuhn, 2016)). Transformed data were then analysed using a one-way analysis of variance (ANOVA) for each parameter measured. Where statistical differences were detected, a TukeyHSD *post-hoc* test was employed at a significance level of $P < 0.05$ (*agricolae* package (de Menibus, 2015)). FA profiles (mg g lipid^{-1}) were also analysed using a linear discriminant analysis (LDA), in order to visualize the relationships between colony position (*MASS* package (Venables & Ripley, 2002)). An LDA biplot was included to show the top fifteen FA driving the differences between colony position. The colour gradient of the vectors show percentage contribution to LDA loadings. Ellipses show 95% confidence intervals. Figures were prepared using the *ggplot2* package (Wickham, 2009).

Results

Proximate composition and zooxanthellae density

Within the size classes, there were no significant differences in total lipid ($P>0.05$) (mg g sample^{-1}) (Fig. 2a), although both edge positions contained lower lipid compared to the next, immediate position. A similar trend was apparent in zooxanthellae densities for the larger colonies (cells cm^{-2}) (Fig. 2e), whereby the density at the edge was again lower than the next immediate position, L-66. On the other hand, the smaller colonies recorded significantly lower zooxanthellae densities at the edge in comparison to the centre ($P<0.05$).

Within both size classes, there was a progressive increase in protein from the centre of the colony toward the edge (mg g sample^{-1}) (Fig. 2b). For the larger colonies, protein at the edge was significantly higher than the centre, while for the smaller colonies, the edge was significantly higher than the centre and S-50 position ($P<0.05$).

The caloric enthalpies showed that, for both size classes, the edge and next immediate position contained the highest energy contents, while the S-centre and L-centre and L-33 positions were low (Fig. 2f). Interestingly, the smaller colonies contained higher overall energy contents in all positions compared to the larger colonies.

Lipid class composition

The proportion of storage lipid in the larger colonies followed a similar trend to the total lipid, with the L-66 position containing the highest amount of storage lipids (WAX, TAG, FFA, and 1,2-DAG), although this was not statistically significant (mg g lipid^{-1}) (Fig. 3a). Similarly, in the

215 smaller colonies, the edge recorded the lowest concentration of storage lipid, and this was
216 significant compared to the S-centre and S-50 positions ($P < 0.05$) (Fig. 3b).

217 The individual lipid class means were similar between the edge positions of the two colony sizes,
218 despite high variability between replicates (Table 1). However, the centre position of each size
219 class was quite different, with the S-centre containing almost two-fold the concentration of TAG
220 compared to the L-centre (S-centre: 499 ± 94.1 and L-centre: 270 ± 123 mg g lipid⁻¹), which
221 translated into markedly higher concentrations of total storage lipid (Fig. 3). The highest TAG
222 concentration in the larger colonies was recorded at L-66. For the smaller colonies, the highest
223 TAG concentration was in the centre. AMPL was significantly higher at S-edge in comparison to
224 the centre and S-50. For the larger colonies, the highest AMPL concentrations were found at the
225 edge and L-33 positions, which were significantly higher than the L-66 ($P < 0.05$).

226

227 **Fatty acid and fatty alcohol composition**

228 In both size classes, the edge contained the lowest concentration of total FA (S-edge: 347 ± 58.6
229 mg g lipid⁻¹ and L-edge: 382 ± 52.6 mg g lipid⁻¹) (Table 2). In the smaller colonies, the highest
230 total FA were found in the centre (519 ± 75.1 mg g lipid⁻¹), while the larger colonies contained
231 the highest total FA in the L-66 position (547 ± 66 mg g lipid⁻¹). These trends extended to the
232 individual FA (mg g lipid⁻¹). Notably, DHA showed a distal decrease from the centre to the edge
233 in the smaller colonies (S-centre: 16.9 ± 3.02 mg g lipid⁻¹ – S-edge: 11.1 ± 2.29 mg g lipid⁻¹), yet
234 in the larger colonies was found in the highest concentrations in the L-66 position (17 ± 2.47 mg
235 g lipid⁻¹), and the lowest in the L-33 and edge positions (~ 12 mg g lipid⁻¹). This was mirrored in

the total PUFA concentrations for both size classes. ARA was an exception, being present in the highest concentrations at the edge, regardless of size class.

When viewed on the basis of % FA, the edge positions recorded significantly higher PUFA concentrations compared to all other positions for the smaller colonies, and compared to the centre and L-66 position for the larger colonies (Table 3) ($P < 0.05$). The edge positions also contained the lowest saturated fatty acids (SFA) concentrations, and this was significant compared to the centre and L-66 positions for the larger colonies ($P < 0.05$).

In the LDA of the FA composition (mg g lipid^{-1}), the first two linear discriminates explained 83.3 % of the total variation between size classes and colony positions (Fig. 4a), with an established Wilks value of 0.0004. The analysis showed a clear difference between the smaller and larger colonies, with the smaller colonies grouping mostly on the positive side of LD1 and negative side of LD2, and the larger showing the inverse. Despite this separation, both size classes followed the same trends. There was clear separation of the edge positions from centre positions. The middle regions (S-50, L-33, L-66) largely grouped between their respective centre and edge positions. The overlapping of the S-centre and S-50 groups illustrates the similarity between these positions, as well as for the L-33, L-66, and L-centre positions.

The LDA biplot (Fig. 4b) shows that the separation of the size classes was largely due to 18 DMA for the small colonies, while 22:6n-3 (DHA), 16:1n-7, and 18:n-6 drove the separation of the larger colonies. Separation of the two edge positions was strongly influenced by the polyunsaturated fatty acids (PUFA) 18:3n-6, 20:5n-3 (EPA), and 20:4n-6 (ARA) as well as the SFA 14:0 and 20:0, and the monounsaturated fatty acid (MUFA), 18:1n-9. Meanwhile, the centre positions were largely influenced by 16:0, 22:4n-6, 20:1n-11, and 20:3n-6.

258

259 Discussion

260 The present study examined the biochemical composition along the longitudinal radius of *A.*
 261 *millepora* colonies, providing a unique account of the compartmentalisation of nutritional
 262 reserves stemming from branch position and functional specialisation within a single coral
 263 colony. These findings provide new insights into colony-wide zonation of the comprehensive
 264 nutritional profile from a length-wise (i.e. colony centre-edge) perspective since, until now,
 265 previous studies have been limited to individual coral branches from a height-wise (i.e. branch
 266 base-tip) perspective (Taylor, 1977; Fang, Chen & Chen, 1989; Gladfelter, Michel & Sanfelici,
 267 1989; Oku et al., 2002; Tang et al., 2015). Since growth of branching scleractinian corals is
 268 characterised by radiate skeletal accretion, the colony edges generally undergo the greatest
 269 growth rates (Kaandorp, 1995). Correspondingly, both colony size classes recorded a distal
 270 increase in total protein from the centre regions toward the edge (Fig. 2b). High protein levels are
 271 characteristic of actively growing sites, where the synthesis and retention of proteins facilitates
 272 calcification, the production of new tissue and polyps, and increased mitotic rates (Ramos-Silva
 273 et al., 2013, 2014). Furthermore, increased production of specialised proteins, such as
 274 mitochondrial respiratory proteins, are necessary to fuel the higher metabolic rates, particularly
 275 respiration, that are stimulated by cell proliferation in corals (Gladfelter, Michel & Sanfelici,
 276 1989; Oku et al., 2002; Hemond, Kaluziak & Vollmer, 2014). These results agree well with
 277 previous studies on the nutritional profile of individual coral branches (base-tip), which showed
 278 an increase in protein concentration at the actively growing tip, compared to the established base
 279 (Oku et al., 2002; Tentori & Allemand, 2006; Tentori & Thomson, 2008). However, these results
 280 show that when individual branches are analysed as a whole, the mean protein concentrations of

each branch position manifests in a nutritional gradient from the colony centre toward the edge that is parallel to that of an individual branch from the base toward the tip. This indicates that a scleractinian coral colony exhibits similar nutritional gradients in two dimensions; height-wise (i.e. base-tip) and length-wise (i.e. centre-edge), and that the latter trend is manifestly stronger than the former.

The regional trend in zooxanthellae densities differed between the two coral size classes (Fig. 2e). The smaller colonies showed a decline in zooxanthellae density from the centre position towards the edge, which was significant. Low zooxanthellae densities at the colony edge is again comparable to growing branch tips, where newly formed tissues are yet to be fully colonised by symbionts (Goreau, 1959; Gladfelter, Michel & Sanfelici, 1989), further demonstrating the similarities between height-wise and length-wise gradients within a coral colony. In contrast, no significant differences were evident in the zooxanthellae densities between regions in the larger colonies. Indeed, the lowest zooxanthellae densities in the larger colonies were akin to the most dense region in the smaller colonies, possibly due to their larger size, as larger coral colonies are suggested to undergo more rapid zooxanthellae proliferation compared to smaller colonies (Muscatine, McCloskey & Loya, 1985).

Although zooxanthellae densities are directly correlated with lipid concentrations in corals (Fang, Chen & Chen, 1989), the lower density at the S-edge did not correlate with low total lipid, in fact, no significant differences were detected between positions for either of the size classes examined. This may suggest an increase in heterotrophic feeding by the edge regions to supplement the reduced phototrophic supply of nutrients (Lesser, 2012; Levas et al., 2015). This is supported by the increased protein concentrations at the edge, since exogenous food sources are known to supply nitrogen-rich building blocks needed for tissue and skeletal biosynthesis

(Osinga et al., 2011). Alternatively, this may indicate intracolony translocation of lipids from the established, zooxanthellae-dense regions of the colony toward the colony edge (Gateno et al., 1998; Parrin et al., 2010). Inner colony regions generally acquire a surplus of energy reserves, since photosynthesis greatly exceeds respiration and competitive interactions are reduced (Gladfelter, Michel & Sanfelici, 1989; Lirman, 2000a). As such, energy accumulated by the inner regions can be mobilised via the coral's gastrovascular system and concentrated in zones of maximal energetic demand, such as the growing edge (Oren, Brickner & Loya, 1998; Bone & Keough, 2010; Marfenin, 2015).

Although the quantity of lipids did not significantly differ between colony positions, there were marked differences in the chemical structure of lipids. In both the size classes examined, the edge contained lower storage lipid compared to the next immediate position. Storage lipids (WAX, TAG, FFA, and 1,2-DAG) are generally associated with energy supply, while structural lipids (ST, AMPL, PE, PS-PI, and PC) are important constituents of the membrane lipid bilayer, where they facilitate cell membrane fluidity, dictate cell permeability, and perform vital cell signalling processes (Lee, Hagen & Kattner, 2006; Ferrier-Pagès et al., 2016). As such, decreased storage lipid at the edges may reflect lipid catabolism to supply the energy demanded by proliferating cells (Oku et al., 2002; Denis et al., 2013). Concurrently, the increased proportion of structural lipids likely reflects tissue synthesis, since ST and phospholipids constitute the building blocks of cell membranes (Imbs et al., 2010).

In the smaller colonies, similar concentrations of storage lipids were found in the centre and S-50 positions. In contrast, the total storage lipid of the larger colony inner regions, namely the centre and L-33 positions, were comparable to the edge (Fig. 3), with the L-66 position containing the highest concentration, largely in the form of TAG. This may suggest a shift in function of the

inner regions of the larger colonies, such that they have transitioned from nutrient assimilation to nutrient remobilisation - allowing the rest of the colony to benefit from their accumulated reserves, as has been shown in colonial plants (Avila-Ospina et al., 2014). This is supported by the energy contents of the L-centre and L-33 positions, which were the lowest of the larger colonies (Fig. 2f). Interestingly, although the combustion enthalpy for protein (23.9 J mg^{-1}) is far lower than lipid (39.5 J mg^{-1}) (Gnaiger & Bitterlich, 1984), the very high levels of protein at the edges manifested in energy levels similar to the positions containing the maximum lipid concentrations, demonstrating the substantial allocation of metabolic resources to colony growth (Ramos-Silva et al., 2014). In addition, the lowest energy content of the smaller colonies was akin to the highest of the larger colonies. This likely reflects the energy-draining effect of attaining a large colony size, since additional material and energy must be invested into the maintenance of existing framework, in addition to ongoing framework construction (Jokiel & Morrissey, 1986). The trends between the smaller and larger colonies extended to the quantitative concentration of total FA (mg g lipid^{-1}). This is illustrated in Fig. 4, which shows that, firstly, there is a clear separation of the two size classes, and, secondly, the trends between colony positions are similar (Fig. 4). The larger colonies show a clear separation between the centre and edge, with the L-33 and L-66 positions bridging the two. Meanwhile, the smaller colonies show high similarity between the centre and S-50 positions, while there is also some similarity between the S-centre, S-50, and L-66 positions.

In both size classes, the edge contained the lowest concentration of total FA, while the highest concentrations were found in the centre and S-50 position for the smaller colonies, and the L-66 position for the larger colonies (Table 2). This conforms to the lipid class results in these positions, which contained higher concentrations of TAG, which comprises three esterified FA,

while the edge is higher in phospholipids and ST, which possess two or less esterified FA (Lee, Hagen & Kattner, 2006). The total FA trends were reflected in the concentrations of most individual FA and confirm that these positions, along with the edges, represent the major energy sinks in their respective colony sizes.

Notably, the S-centre, S-50, and L-66 positions all exhibited higher SFA and MUFA concentrations, largely in the form of 14:0, 16:0, and 18:1n-9 (Table 2). These represent FA that are known to be energy-rich and readily catabolised, and are largely derived from zooxanthellae, corresponding to the zooxanthellae results of these positions (Figueiredo et al., 2012).

Furthermore, large reserves of energy-rich lipid constituents, including TAG, SFA, and MUFA, are typically associated with coral reproduction; an energetically expensive life process (Figueiredo et al., 2012). Since corals must partition metabolic energy amongst several important physiological processes (Leuzinger, Willis & Anthony, 2012), the predominance of these compounds in the L-66, S-centre, and S-50 positions implicate these regions as being reproductively active. This correlates with the findings of Nozawa & Lin (2014), who showed that polyps obtained from the L-50 position of large *Acropora hyacinthus* colonies had the highest fecundity levels, while the highest fecundity was detected in the centre and S-50 positions of smaller colonies.

In contrast, the edge positions were conspicuously low in these readily catabolised materials, conforming to both the lower zooxanthellae densities and the well-documented sterility of actively growing regions in *Acropora* colonies (Hemond, Kaluziak & Vollmer, 2014; Nozawa & Lin, 2014). Correspondingly, the edges contained the highest proportions of PUFA (% FA), which are known to be major constituents of cell membranes and are required for high growth and development rates (Brett & Muller-Navara, 1997; Sargent et al., 1999a). Interestingly,

arachidonic acid (20:4n-6, ARA) was one of few FA to exhibit higher concentrations at the colony edge, regardless of size class (mg g lipid⁻¹). ARA is known to play a significant role in eicosanoid production, growth, morphogenesis, regeneration, and budding in cnidarian tissues, which corresponds to its higher quantity at the edges (Pierobon et al., 1997; Tang et al., 2015). Furthermore, this may reflect demand for ARA-rich immune cells to fight surface-associated bacteria in newly-colonised surfaces (Pernet, Bricelj & Parrish, 2005). Bolstered immunity is particularly important for branches at the colony edge, which are more vulnerable to external stressors such as parasites and pathogens (D'Angelo et al., 2012). Indeed, it has been shown that progressive mortality generally begins from the colony edge in response to stressors such as poor water quality (Kuntz et al., 2005) and disease (Weil, Cróquer & Urreiztieta, 2009; D'Angelo et al., 2012). Once again, the origin of this FA is unknown - higher ARA may signify increased heterotrophy (Dodds et al., 2009), increased FA biosynthesis, or intracolony transport from the inner regions (Gateno et al., 1998). Regardless of the acquisition method, these results clearly show that the scleractinian coral colony is not nutritionally homogeneous (Tentori & Thomson, 2008; Osinga et al., 2012). While different regions of the colony are functionally specialised for specific roles, so too are their nutritional profiles different, demonstrating tight integration of a single coral colony such that, while individual regions must undergo a trade-off for resource allocation, the colony as a whole is able to undergo several important life functions at once.

These results also provide fundamental information for prudent harvesting strategies of wild donor coral colonies to generate stock for the purposes of aquaculture, the aquarium trade (Olivotto et al., 2011; Leal et al., 2016), and translocation to degraded reef sites (Miyazaki, Keshavmurthy & Funami, 2010; Toh et al., 2013). Fragmentation and translocation of corals is inevitably a highly stressful event, and the speed at which recovery occurs is critical to survival

and ongoing health (Lirman, 2000b; Roff, Hoegh-Guldberg & Fine, 2006). Since storage lipids and their constituent FA represent important energy reserves during stressful periods for coral (Imbs & Yakovleva, 2011; Denis et al., 2013), judicious selection of branches inherently rich in these compounds will maximise their survival and recovery prospects. Indeed, it has previously been shown that there is a significant, inverse relationship between initial coral lipid stores and the timing of the onset of high mortality rates following major stress events (Anthony et al., 2009). Concordantly, branches undergoing rapid growth, which contain lower storage lipid reserves, have previously been shown to exhibit lowered regenerative capacities (Oren et al., 2001; Roff, Hoegh-Guldberg & Fine, 2006; Denis et al., 2013). In consideration of this, the results of the present study suggest that the L-66 position of the larger size class ($4376 \pm 741 \text{ cm}^2$), and the S-centre and S-50 positions of the smaller size class ($1410 \pm 88 \text{ cm}^2$), are metabolically active branches containing large stores of energy-rich lipids and not undergoing rapid growth - thus representing positions with the greatest survival and health prospects following fragmentation and translocation.

411 **Acknowledgements:**

412 This project was funded by the Australian Institute of Marine Science (AIMS) and Deakin
 413 University. The authors thank the SeaSim team at AIMS and the staff of Deakin University's
 414 School of Life and Environmental Sciences for technical assistance throughout the project. This
 415 work conforms to the legal requirements of Australia.

References

- Anthony KRN., Connolly SR., Willis BL. 2002. Comparative analysis of energy allocation to tissue and skeletal growth in corals. *Limnology and Oceanography* 47:1417–1429. DOI: 10.4319/lo.2002.47.5.1417.
- Anthony KRN., Hoogenboom MO., Maynard JA., Grottoli A., Middlebrook R. 2009. Energetics approach to predicting mortality risk from environmental stress: A case study of coral bleaching. *Functional Ecology* 23:539–550. DOI: 10.1111/j.1365-2435.2008.01531.x.
- Arvedlund M., Craggs J., Pecorelli J. 2003. Coral Culture — Possible Future Trends and Directions. In: Cato J, Brown C eds. *Marine Ornamental Species: Collection, Culture and Conservation*. Iowa State Press,.
- Avila-Ospina L., Moison M., Yoshimoto K., Masclaux-Daubresse C. 2014. Autophagy, plant senescence, and nutrient recycling. *Journal of Experimental Botany* 65:3799–3811. DOI: 10.1093/jxb/eru039.
- Bone EK., Keough MJ. 2010. Does polymorphism predict physiological connectedness? A test using two encrusting bryozoans. *Biological Bulletin* 219:220–230.
- Brett M., Muller-Navara D. 1997. The role of highly unsaturated fatty acids in aquatic foodweb processes. *Freshwater Biology* 38:483–499.
- Conlan J., Jones P., Turchini G., Hall M., Francis D. 2014. Changes in the nutritional composition of captive early-mid stage *Panulirus ornatus* phyllosoma over ecdysis and larval development. *Aquaculture* 434:159–170.
- Conlan JA., Rocker MM., Francis DS. 2017. A comparison of two common sample preparation techniques for lipid and fatty acid analysis in three different coral morphotypes reveals quantitative and qualitative differences. *PeerJ* 5:e3645. DOI: 10.7717/peerj.3645.
- D’Angelo C., Smith EG., Oswald F., Burt J., Tchernov D., Wiedenmann J. 2012. Locally accelerated growth is part of the innate immune response and repair mechanisms in reef-building corals as detected by green fluorescent protein (GFP)-like pigments. *Coral Reefs* 31:1045–1056. DOI: 10.1007/s00338-012-0926-8.
- Denis V., Guillaume MMM., Goutx M., de Palmas S., Debreuil J., Baker AC., Boonstra RK., Bruggemann JH. 2013. Fast growth may impair regeneration capacity in the branching coral *Acropora muricata*. *PloS one* 8:e72618. DOI: 10.1371/journal.pone.0072618.
- Dodds L a., Black KD., Orr H., Roberts JM. 2009. Lipid biomarkers reveal geographical differences in food supply to the cold-water coral *Lophelia pertusa* (Scleractinia). *Marine Ecology Progress Series* 397:113–124. DOI: 10.3354/meps08143.
- Fang LS., Chen Y., Chen CS. 1989. Why does the white tip of stony coral grow so fast without zooxanthellae? *Marine Biology* 103:359–363.
- Ferrier-Pagès C., Godinot C., D’Angelo C., Wiedenmann J., Grover R. 2016. Phosphorus metabolism of reef organisms with algal symbionts. *Ecological Monographs* 86:262–277. DOI: 10.1002/ecm.1217.

- 454 Figueiredo J., Baird AH., Cohen MF., Flot J-FF., Kamiki T., Meziane T., Tsuchiya M.,
455 Yamasaki H. 2012. Ontogenetic change in the lipid and fatty acid composition of
456 scleractinian coral larvae. *Coral Reefs* 31:613–619. DOI: 10.1007/s00338-012-0874-3.
- 457 Forsman Z., Page CA., Toonen RJ., Vaughan D. 2015. Growing coral larger and faster: micro-
458 colony-fusion as a strategy for accelerating coral cover. *PeerJ* 3:e1313. DOI:
459 10.7717/peerj.1313.
- 460 Gateno D., Israel A., Barki Y., Rinkevich B. 1998. Gastrovascular circulation in an octocoral:
461 Evidence of significant transport of coral and symbiont cells. *Biological Bulletin* 194:178–
462 186. DOI: 10.2307/1543048.
- 463 Gladfelter EH., Michel G., Sanfelici A. 1989. Metabolic gradients along a branch of the reef
464 coral *Acropora palmata*. *Bulletin of Marine Science* 44:1166–1173.
- 465 Gnaiger E., Bitterlich G. 1984. Proximate biochemical composition and caloric content
466 calculated from elemental CHN analysis: a stoichiometric concept. *Oecologia* 62:289–298.
467 DOI: 10.1007/BF00384259.
- 468 Goreau T. 1959. The physiology of skeleton formation in corals. I. A method for measuring the
469 rate of calcium deposition by corals under different conditions. *Biological Bulletin* 116:59–
470 75.
- 471 Hemond EM., Kaluziak ST., Vollmer S V. 2014. The genetics of colony form and function in
472 Caribbean *Acropora* corals. *BMC genomics* 15:1133. DOI: 10.1186/1471-2164-15-1133.
- 473 Houlbrèque F., Ferrier-Pagès C. 2009. Heterotrophy in tropical scleractinian corals. *Biological*
474 *reviews of the Cambridge Philosophical Society* 84:1–17. DOI: 10.1111/j.1469-
475 185X.2008.00058.x.
- 476 Hughes RN. 2005. Lessons in modularity: the evolutionary ecology of colonial invertebrates.
477 *Scientia Marina* 69:169–179. DOI: 10.3989/scimar.2005.69s1169.
- 478 Imbs AB. 2013. Fatty acids and other lipids of corals: Composition, distribution, and
479 biosynthesis. *Russian Journal of Marine Biology* 39:153–168. DOI:
480 10.1134/S1063074013030061.
- 481 Imbs AB., Latyshev N., Dautova T., Latypov Y. 2010. Distribution of lipids and fatty acids in
482 corals by their taxonomic position and presence of zooxanthellae. *Marine Ecology Progress*
483 *Series* 409:65–75. DOI: 10.3354/meps08622.
- 484 Imbs AB., Yakovleva IM. 2011. Dynamics of lipid and fatty acid composition of shallow-water
485 corals under thermal stress: an experimental approach. *Coral Reefs* 31:41–53. DOI:
486 10.1007/s00338-011-0817-4.
- 487 Jokiel PL., Morrissey JI. 1986. Influence of size on primary production in the reef coral
488 *Pocillopora damicornis* and the macroalga *Acanthophora spicifera*. *Marine Biology* 91:15–
489 26.
- 490 Kaandorp JA. 1995. Analysis and synthesis of radiate accretive growth in three dimensions.
491 *Journal of theoretical biology* 175:39–55. DOI: 10.1006/jtbi.1995.0119.

- 492 Kuhn M. 2016. caret: Classification and Regression Training.
- 493 Kuntz NM., Kline DI., Sandin SA., Rohwer F. 2005. Pathologies and mortality rates caused by
494 organic carbon and nutrient stressors in three Caribbean coral species. *Marine Ecology*
495 *Progress Series* 294:173–180. DOI: 10.3354/meps294173.
- 496 Leal MC., Ferrier-Pagès C., Petersen D., Osinga R. 2016. Coral aquaculture: applying scientific
497 knowledge to *ex situ* production. *Reviews in Aquaculture* 6:1–18. DOI: 10.1111/raq.12087.
- 498 Lee RF., Hagen W., Kattner G. 2006. Lipid storage in marine zooplankton. *Marine Ecology*
499 *Progress Series* 307:273–306.
- 500 Lesser MP. 2012. Using energetic budgets to assess the effects of environmental stress on corals:
501 are we measuring the right things? *Coral Reefs* 32:25–33. DOI: 10.1007/s00338-012-0993-
502 x.
- 503 Leuzinger S., Anthony KRN., Willis BL. 2003. Reproductive energy investment in corals:
504 scaling with module size. *Oecologia* 136:524–31. DOI: 10.1007/s00442-003-1305-5.
- 505 Leuzinger S., Willis BL., Anthony KRN. 2012. Energy allocation in a reef coral under varying
506 resource availability. *Marine Biology* 159:177–186. DOI: 10.1007/s00227-011-1797-1.
- 507 Levas S., Grottoli AG., Schoepf V., Aschaffenburg M., Baumann J., Bauer JE., Warner ME.
508 2015. Can heterotrophic uptake of dissolved organic carbon and zooplankton mitigate
509 carbon budget deficits in annually bleached corals? *Coral Reefs*:1–12. DOI:
510 10.1007/s00338-015-1390-z.
- 511 Lirman D. 2000a. Lesion regeneration in the branching coral *Acropora palmata*: Effects of
512 colonization, colony size, lesion size, and lesion shape. *Marine Ecology Progress Series*
513 197:209–215. DOI: 10.3354/meps197209.
- 514 Lirman D. 2000b. Fragmentation in the branching coral *Acropora palmata* (Lamarck): growth,
515 survivorship, and reproduction of colonies and fragments. *Journal of Experimental Marine*
516 *Biology and Ecology* 251:41–57. DOI: 10.1016/S0022-0981(00)00205-7.
- 517 Mackie G. 1986. From aggregates to integrates, physiological aspects of modularity in colonial
518 animals. *Phil. Trans. R. Soc. Lond.* 313:175–196.
- 519 Marfenin N. 2015. Non-radial symmetry of the transport system of *Acropora* corals. *Invertebrate*
520 *Zoology* 12:53–59.
- 521 de Meniburu F. 2015. agricolae: Statistical procedures for agricultural research.
- 522 Miyazaki K., Keshavmurthy S., Funami K. 2010. Survival and growth of transplanted coral
523 fragments in a high-latitude coral community (32 deg N) in Kochi, Japan. *Kuroshio*
524 *Biosphere* 6:1–9.
- 525 Muscatine L. 1990. The role of symbiotic algae in carbon and energy flux in coral reefs. In:
526 *Ecosystems of the world*. 75–87.
- 527 Muscatine L., McCloskey L., Loya Y. 1985. A comparison of the growth rates of zooxanthellae
528 and animal tissue. *Proceedings of the fifth international coral reef congress, Tahiti* 6:119–
529 123.

- 530 Nakamura T., Yamasaki H. 2006. Morphological changes of pocilloporid corals exposed to
531 water flow. *Proceedings of the 10th International Coral Reef ...* 875:872–875.
- 532 Naumann MS., Niggel W., Laforsch C., Glaser C., Wild C. 2009. Coral surface area
533 quantification-evaluation of established techniques by comparison with computer
534 tomography. *Coral Reefs* 28:109–117. DOI: 10.1007/s00338-008-0459-3.
- 535 Nozawa Y., Lin CH. 2014. Effects of colony size and polyp position on polyp fecundity in the
536 scleractinian coral genus *Acropora*. *Coral Reefs*:1057–1066. DOI: 10.1007/s00338-014-
537 1185-7.
- 538 Oku H., Yamashiro H., Onaga K., Iwasaki H., Takara K. 2002. Lipid distribution in branching
539 coral *Montipora digitata*. *Fisheries Science* 68:517–522. DOI: 10.1046/j.1444-
540 2906.2002.00456.x.
- 541 Olivotto I., Planas M., Simões N., Holt GJ., Avella MA., Calado R. 2011. Advances in Breeding
542 and Rearing Marine Ornamentals. *Journal of the World Aquaculture Society* 42:135–166.
543 DOI: 10.1111/j.1749-7345.2011.00453.x.
- 544 Oren U., Benayahu Y., Lubinevsky H., Loya Y. 2001. Colony Integration during Regeneration in
545 the Stony Coral *Favia fava*. *Ecology* 82:802–813.
- 546 Oren U., Brickner I., Loya Y. 1998. Prudent sessile feeding by the corallivore snail,
547 *Coralliophila violacea* on coral energy sinks. *Proceedings of the Royal Society B:*
548 *Biological Sciences* 265:2043–2050. DOI: 10.1098/rspb.1998.0538.
- 549 Oren U., Rinkevich B., Loya Y. 1997. Oriented intra-colonial transport of ¹⁴C labeled materials
550 during coral regeneration. *Marine Ecology Progress Series* 161:117–122. DOI:
551 10.3354/meps161117.
- 552 Osinga R., Schutter M., Griffioen B., Wijffels RH., Verreth JAJ., Shafir S., Henard S., Taruffi
553 M., Gili C., Lavorano S. 2011. The biology and economics of coral growth. *Marine*
554 *Biotechnology* 13:658–671. DOI: 10.1007/s10126-011-9382-7.
- 555 Osinga R., Schutter M., Wijgerde T., Rinkevich B., Shafir S., Shpigel M., Luna GM., Danovaro
556 R., Bongiorno L., Deutsch A., Kuecken M., Hiddinga B., Janse M., McLeod A., Gili C.,
557 Lavorano S., Henard S., Barthelemy D., Westhoff G., Baylina N., Santos E., Weissenbacher
558 A., Kuba M., Jones R., Leewis R., Petersen D., Laterveer M. 2012. The CORALZOO
559 project: a synopsis of four years of public aquarium science. *Journal of the Marine*
560 *Biological Association of the United Kingdom* 92:753–768. DOI:
561 10.1017/S0025315411001779.
- 562 Parrin AP., Netherton SE., Bross LS., McFadden CS., Blackstone NW. 2010. Circulation of
563 fluids in the gastrovascular system of a stoloniferan octocoral. *Biological Bulletin* 219:112–
564 121. DOI: 219/2/112 [pii].
- 565 Parrish CC., Bodennec G., Gentien P. 1996. Determination of glycolipids by Chromarod
566 thin-layer chromatography with Iatroscan flame ionization detection. *Journal of*
567 *Chromatography* 741:91–97.
- 568 Pernet F., Bricelj VM., Parrish CC. 2005. Effect of varying dietary levels of n-6 polyunsaturated
569 fatty acids during the early ontogeny of the sea scallop, *Placopecten magellanicus*. *Journal*

- 570 *of Experimental Marine Biology and Ecology* 327:115–133. DOI:
571 10.1016/j.jembe.2005.06.008.
- 572 Pierobon P., De Petrocellis L., Minei R., Di Marzo V. 1997. Arachidonic acid as an endogenous
573 signal for the glutathione-induced feeding response in *Hydra*. *Cellular and Molecular Life*
574 *Sciences* 53:61–68. DOI: 10.1007/PL00000580.
- 575 R Development Core Team. 2016. R: A language and environment for statistical computing. R
576 *Foundation for Statistical Computing* Vienna, Au.
- 577 Ramos-Silva P., Kaandorp J., Herbst F., Plasseraud L., Alcaraz G., Stern C., Corneillat M.,
578 Guichard N., Durllet C., Luquet G., Marin F. 2014. The skeleton of the staghorn coral
579 *Acropora millepora*: Molecular and structural characterization. *PLoS ONE* 9. DOI:
580 10.1371/journal.pone.0097454.
- 581 Ramos-Silva P., Kaandorp J., Huisman L., Marie B., Zanella-Cléon I., Guichard N., Miller DJ.,
582 Marin F. 2013. The skeletal proteome of the coral *Acropora millepora*: The evolution of
583 calcification by co-option and domain shuffling. *Molecular Biology and Evolution*
584 30:2099–2112. DOI: 10.1093/molbev/mst109.
- 585 Roff G., Hoegh-Guldberg O., Fine M. 2006. Intra-colonial response to Acroporid “white
586 syndrome” lesions in tabular *Acropora* spp. (Scleractinia). *Coral Reefs* 25:255–264. DOI:
587 10.1007/s00338-006-0099-4.
- 588 RStudio Team. 2015. RStudio: Integrated Development Environment for R.
- 589 Sargent J., Bell G., McEvoy L., Tocher D., Estevez A. 1999a. Recent developments in the
590 essential fatty acid nutrition of fish. *Aquaculture* 177:191–199. DOI: 10.1016/S0044-
591 8486(99)00083-6.
- 592 Sargent J., McEvoy L., Estevez A., Bell G., Bell M., Henderson J., Tocher D. 1999b. Lipid
593 nutrition of marine fish during early development: current status and future directions.
594 *Aquaculture* 179:217–229. DOI: 10.1016/S0044-8486(99)00191-X.
- 595 Schindelin J., Arganda-Carreras I., Frise E., Kaynig V., Longair M., Pietzsch T., Preibisch S.,
596 Rueden C., Saalfeld S., Schmid B., Tinevez J-Y., White DJ., Hartenstein V., Eliceiri K.,
597 Tomancak P., Cardona A. 2012. Fiji: an open-source platform for biological-image analysis.
598 *Nature methods* 9:676–82. DOI: 10.1038/nmeth.2019.
- 599 Sheridan C., Kramarsky-Winter E., Sweet M., Kushmaro A., Leal MC. 2013. Diseases in coral
600 aquaculture: Causes, implications and preventions. *Aquaculture* 396–399:124–135. DOI:
601 10.1016/j.aquaculture.2013.02.037.
- 602 Smith LD., Hughes TP. 1999. An experimental assessment of survival, re-attachment and
603 fecundity of coral fragments. *Journal of Experimental Marine Biology and Ecology*
604 235:147–164. DOI: 10.1016/S0022-0981(98)00178-6.
- 605 Szmant AM., Gassman NJ. 1990. The effects of prolonged “bleaching” on the tissue biomass and
606 reproduction of the reef coral *Montastrea annularis*. *Coral Reefs* 8:217–224. DOI:
607 10.1007/BF00265014.
- 608 Tang CH., Ku PC., Lin CY., Chen TH., Lee KH., Lee SH., Wang WH. 2015. Intra-Colonial

609 Functional Differentiation-Related Modulation of the Cellular Membrane in a Pocilloporid
610 Coral *Seriatopora caliendrum*. *Marine Biotechnology* 17:633–643. DOI: 10.1007/s10126-
611 015-9645-9.

612 Taylor DL. 1977. Intra-colonial transport of organic compounds and calcium in some atlantic
613 reef corals. *Proc. of the 3rd Int. Coral Reef Symp.*:431–436.

614 Tentori E., Allemand D. 2006. Light-enhanced calcification and dark decalcification in isolates
615 of the soft coral *Cladiella* sp. during tissue recovery. *Biological Bulletin* 211:193–202. DOI:
616 10.2307/4134593.

617 Tentori E., Thomson M. 2008. Differential expression of soluble and membrane-bound proteins
618 in soft corals (Cnidaria: Octocorallia). *Marine And Freshwater Research*:7–11.

619 Toh TC., Ng CSL., Guest J., Chou LM. 2013. Grazers improve health of coral juveniles in *ex*
620 *situ* mariculture. *Aquaculture* 414–415:288–293. DOI: 10.1016/j.aquaculture.2013.08.025.

621 Venables WN., Ripley BD. 2002. *Modern Applied Statistics with S*. New York: Springer.

622 Vollmer S V., Edmunds PJ. 2000. Allometric scaling in small colonies of the scleractinian coral
623 *Siderastrea siderea* (Ellis and Solander). *Biological Bulletin* 199:21–28. DOI:
624 10.2307/1542703.

625 Ward S. 1995. Two patterns of energy allocation for growth, reproduction and lipid storage in
626 the scleractinian coral *Pocillopora damicornis*. *Coral Reefs* 14:87–90.

627 Weil E., Cróquer A., Urreiztieta I. 2009. Yellow band disease compromises the reproductive
628 output of the Caribbean reef-building coral *Montastraea faveolata* (Anthozoa, Scleractinia).
629 *Diseases of Aquatic Organisms* 87:45–55. DOI: 10.3354/dao02103.

630 Wickham H. 2009. *ggplot2: Elegant Graphics for Data Analysis*. New York: Springer-Verlag.

631 Figure legends

632 Figure 1

633 Branch sampling locations of *Acropora millepora* colonies. (a) Larger colony ($4376 \pm 741 \text{ cm}^2$), L-centre: colony centre, L-33: 33.3 %
634 of the longitudinal radius length, L-66: 66.6 % of the longitudinal radius length, L-edge: colony edge. (b) Smaller colony (1410 ± 88
635 cm^2), S-centre: colony centre, S-50: 50 % of the longitudinal radius length, S-edge: colony edge (S-edge).

636 Figure 2

637 Proximate composition, energy content, and zooxanthellae density of distal intracolony locations in two size classes of *Acropora*
638 *millepora* colonies. (a) Total lipid concentration, (b) Total protein concentration, (c) Total nitrogen-free extract concentration (NFE),
639 (d) Total ash concentration, (e) Zooxanthellae density, (f) Energy content (using caloric enthalpies of lipid + protein). L-centre: larger
640 colony centre, L-33: 33.3 % of the longitudinal radius length, L-66: 66.6 % of the longitudinal radius length, L-edge: larger colony
641 edge, S-centre: smaller colony centre, S-50: 50 % of the longitudinal radius length, S-edge: smaller colony edge (S-edge). Values are
642 presented as means \pm SEM. Letters in common denote no significant difference ($P < 0.05$).

643 Figure 3

644 Lipid class composition - relative proportion of storage and structural lipids of distal intracolony locations in two size classes of
645 *Acropora millepora* colonies. L-centre: larger colony centre, L-33: 33.3% of the longitudinal radius length, L-66: 66.6% of the

646 longitudinal radius length, L-edge: larger colony edge, S-centre: smaller colony centre, S-50: 50% of the longitudinal radius length, S-
647 edge: smaller colony edge (S-edge). Values are presented as means \pm SEM. Letters in common denote no significant difference
648 ($P < 0.05$).

649 **Figure 4**

650 Linear discriminant analysis (LDA) a) score plot and b) biplot, showing overall fatty acid profile (mg g lipid⁻¹) of distal intracolonic
651 locations in two size classes of *Acropora millepora* colonies. L-centre: larger colony centre, L-33: 33.3% of the longitudinal radius
652 length, L-66: 66.6% of the longitudinal radius length, L-edge: larger colony edge, S-centre: smaller colony centre, S-50: 50% of the
653 longitudinal radius length, S-edge: smaller colony edge (S-edge). a) Ellipses show 95% confidence intervals for each treatment. b)
654 Vectors show top fifteen individual fatty acids and fatty alcohols contributing to the overall variance between treatments. Colour
655 gradient shows percentage contribution to LDA loadings.

Figure 1

Branch sampling locations of *Acropora millepora* colonies.

(a) Larger colony ($4376 \pm 741 \text{ cm}^2$), L-centre: colony centre, L-33: 33.3 % of the longitudinal radius length, L-66: 66.6 % of the longitudinal radius length, L-edge: colony edge. (b) Smaller colony ($1410 \pm 88 \text{ cm}^2$), S-centre: colony centre, S-50: 50 % of the longitudinal radius length, S-edge: colony edge (S-edge).

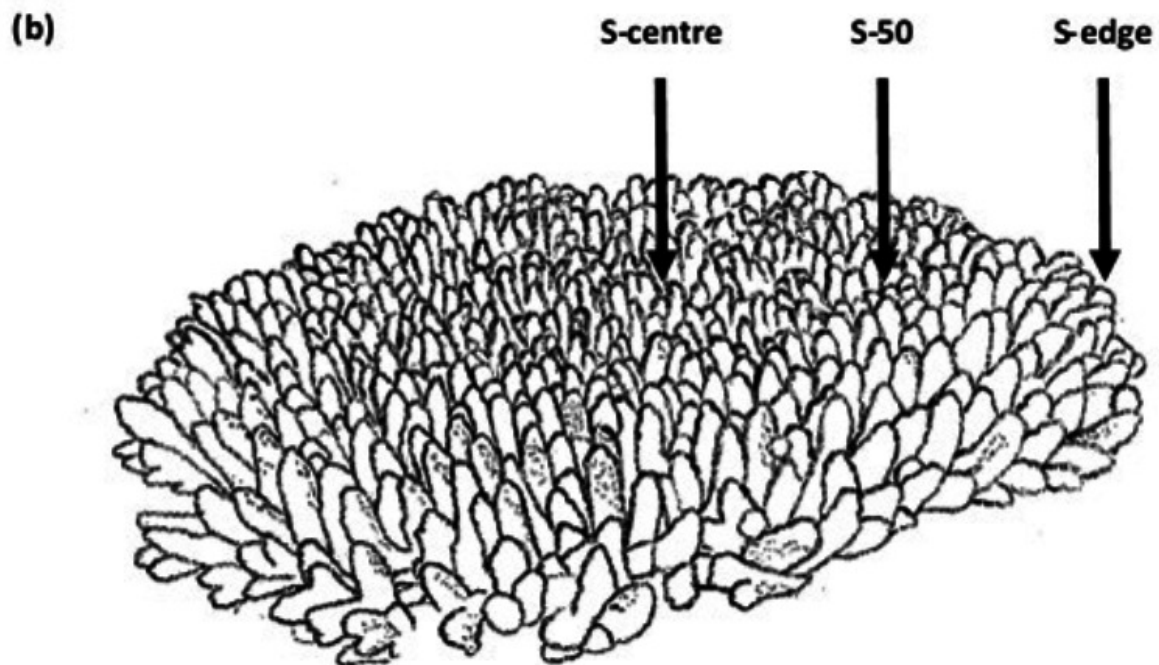
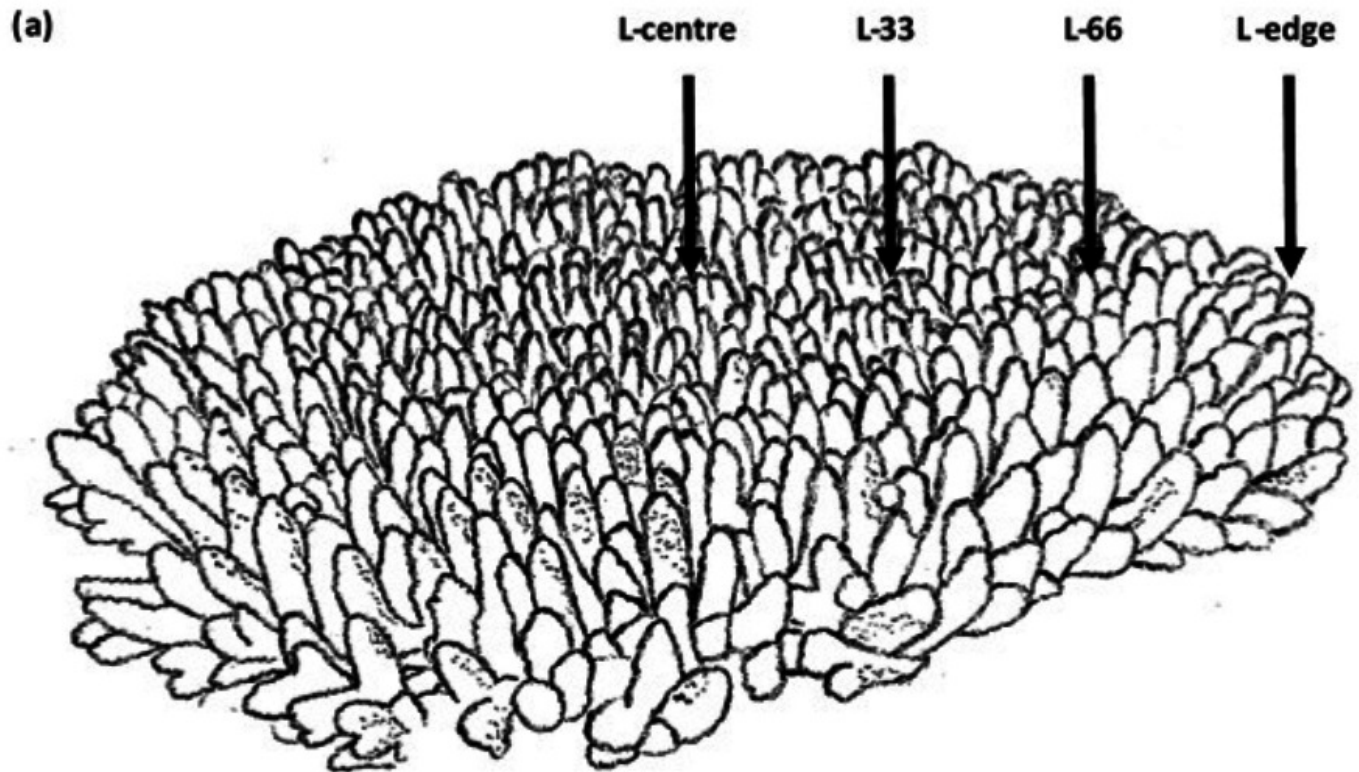


Figure 2

Proximate composition, energy content, and zooxanthellae density of distal intracolony locations in two size classes of *Acropora millepora* colonies.

(a) Total lipid concentration, (b) Total protein concentration, (c) Total nitrogen-free extract concentration (NFE), (d) Total ash concentration, (e) Zooxanthellae density, (f) Energy content (using caloric enthalpies of lipid + protein). L-centre: larger colony centre, L-33: 33.3 % of the longitudinal radius length, L-66: 66.6 % of the longitudinal radius length, L-edge: larger colony edge, S-centre: smaller colony centre, S-50: 50 % of the longitudinal radius length, S-edge: smaller colony edge (S-edge). Values are presented as means \pm SEM. Letters in common denote no significant difference ($P < 0.05$).

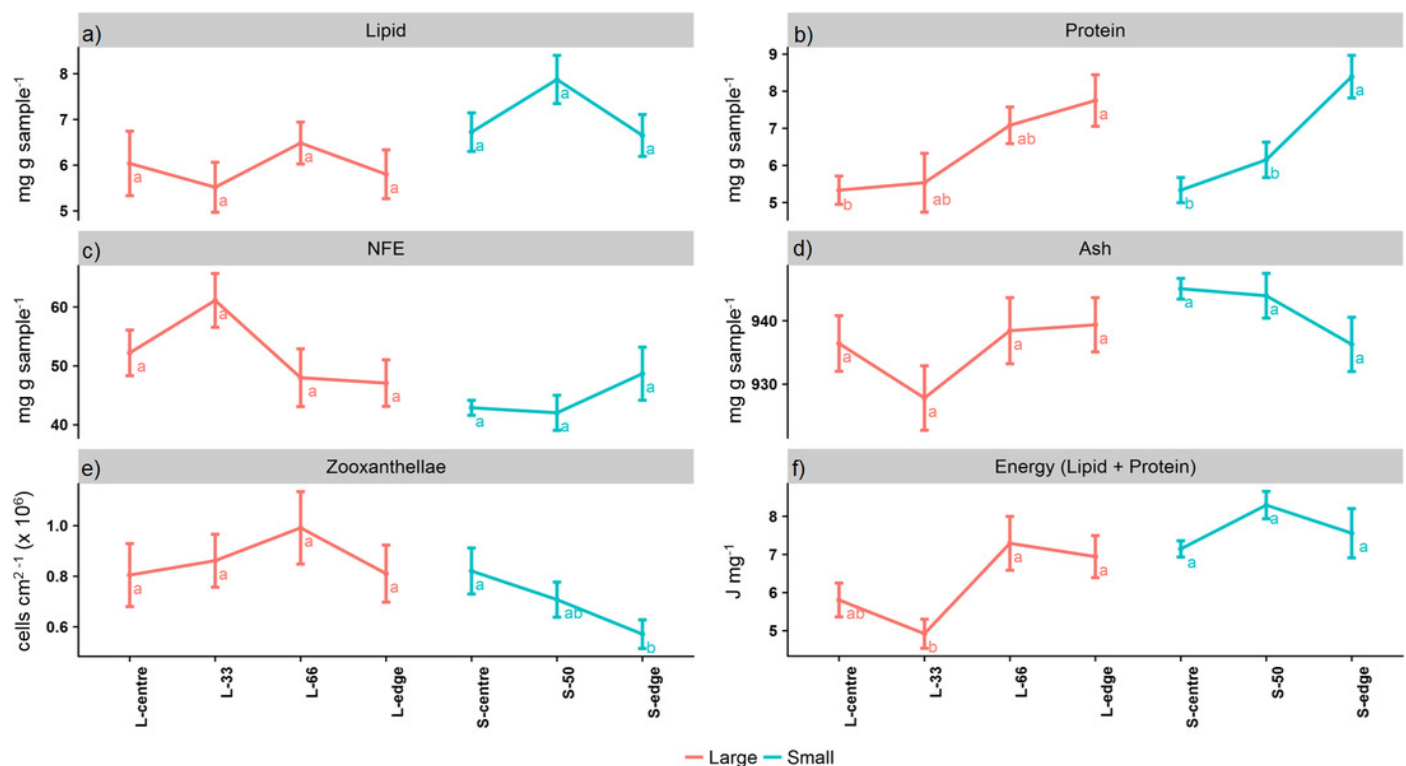


Figure 3

Lipid class composition - relative proportion of storage and structural lipids of distal intracolony locations in two size classes of *Acropora millepora* colonies.

L-centre: larger colony centre, L-33: 33.3% of the longitudinal radius length, L-66: 66.6% of the longitudinal radius length, L-edge: larger colony edge, S-centre: smaller colony centre, S-50: 50% of the longitudinal radius length, S-edge: smaller colony edge (S-edge). Values are presented as means \pm SEM. Letters in common denote no significant difference ($P < 0.05$).

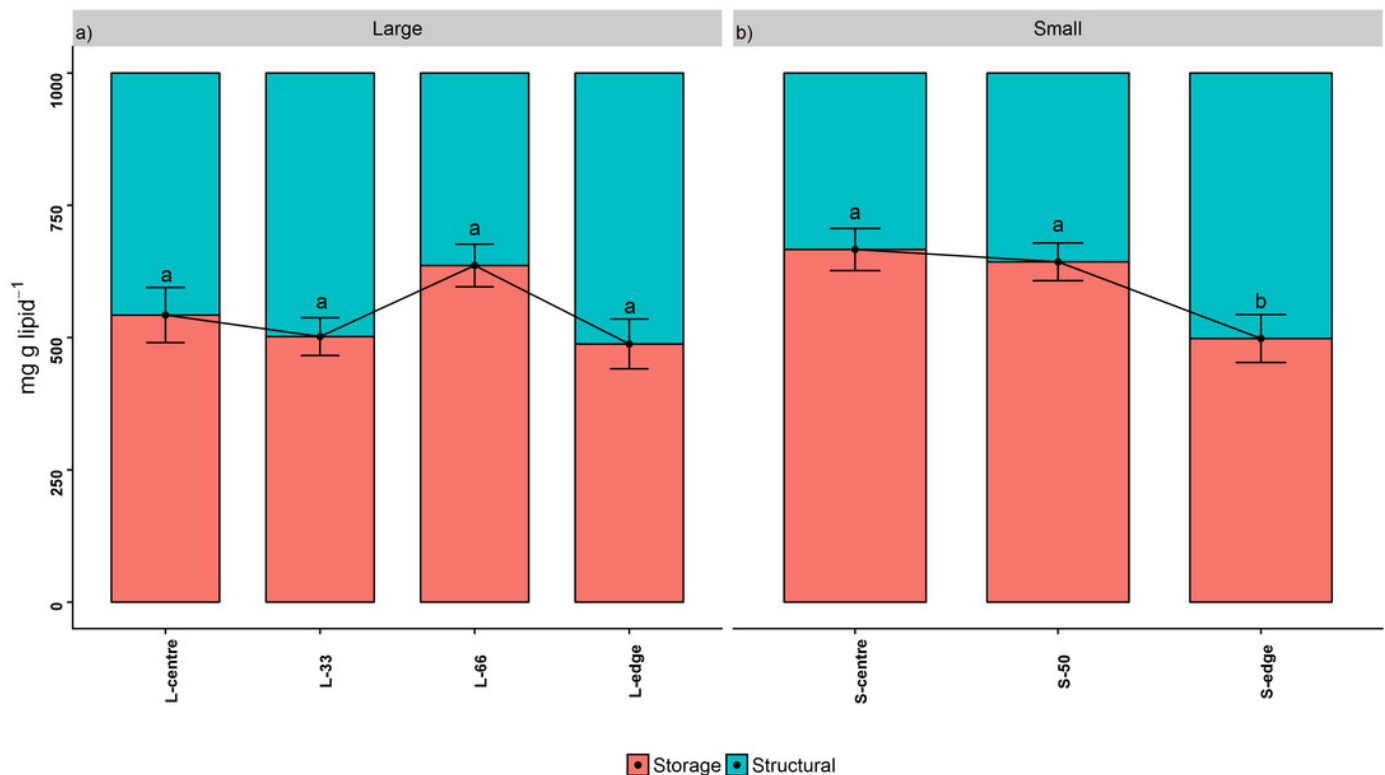


Figure 4

Linear discriminant analysis (LDA) a) score plot and b) biplot, showing overall fatty acid profile (mg g lipid⁻¹) of distal intracolony locations in two size classes of *Acropora millepora* colonies.

L-centre: larger colony centre, L-33: 33.3% of the longitudinal radius length, L-66: 66.6% of the longitudinal radius length, L-edge: larger colony edge, S-centre: smaller colony centre, S-50: 50% of the longitudinal radius length, S-edge: smaller colony edge (S-edge). a) Ellipses show 95% confidence intervals for each treatment. b) Vectors show top fifteen individual fatty acids and fatty alcohols contributing to the overall variance between treatments. Colour gradient shows percentage contribution to LDA loadings.

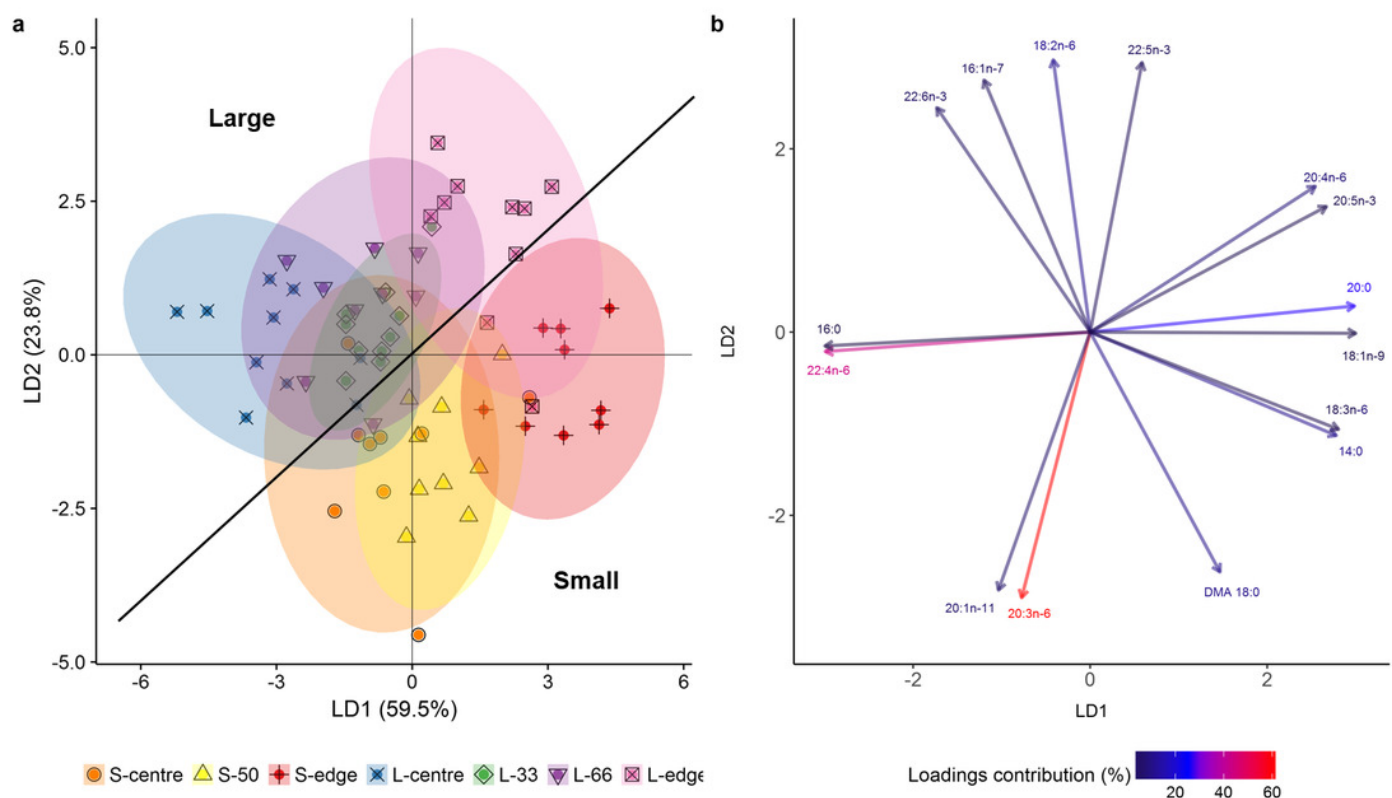


Table 1 (on next page)

Lipid class composition (mg g lipid⁻¹) of distal intracolony locations in two size classes of *Acropora millepora* colonies.

L-centre: large colony centre, L-33: 33.3% of the longitudinal radius length, L-66: 66.6% of the longitudinal radius length, L-edge: large colony edge, S-centre: small colony centre, S-50: 50% of the longitudinal radius length, S-edge: small colony edge (S-edge). Values are presented as means \pm SEM. For each colony size, values in the same row size that do not share the same superscripts are significantly different ($P < 0.05$).

1 *Table 1*

2 Lipid class composition (mg g lipid⁻¹) of distal intracolony locations in two size classes of *Acropora millepora* colonies. L-centre:
3 large colony centre, L-33: 33.3% of the longitudinal radius length, L-66: 66.6% of the longitudinal radius length, L-edge: large colony
4 edge, S-centre: small colony centre, S-50: 50% of the longitudinal radius length, S-edge: small colony edge (S-edge). Values are
5 presented as means ± SEM. For each colony size, values in the same row size that do not share the same superscripts are significantly
6 different ($P<0.05$).

Lipid class (mg g lipid ⁻¹)	Small			Large			
	Centre	S-50	Edge	Centre	L-33	L-66	Edge
Wax ester	114±15.9 ^b	171±48.5 ^a	118±15.8 ^{ab}	194±92.3 ^a	130±7.71 ^a	125±9.88 ^a	119±6.77 ^a
Triacylglycerol	499±94.1 ^a	411±92.8 ^a	311±94.9 ^a	270±123 ^a	301±69.9 ^a	456±69.2 ^a	312±75.3 ^{ab}
Free fatty acid	14.6±3.48 ^a	16.5±5.78 ^a	19±3.29 ^a	20.1±7.05 ^a	18.3±2.73 ^a	17±3.16 ^a	22.2±2.08 ^a
1,2-diacylglycerol	39.1±13 ^a	44.5±13 ^a	50.6±14.5 ^a	58.5±19.4 ^a	52.7±22.1 ^a	38±10.7 ^a	34.5±14 ^a
Sterol	44.9±9.17 ^b	48.5±8.31 ^b	71.9±9.47 ^a	56.4±9.42 ^a	66±7.72 ^a	63.9±28 ^a	74.1±6.81 ^a
AMPL	96.7±23 ^b	100±20.6 ^b	150±25.6 ^a	118±21.3 ^{ab}	138±17 ^a	88.5±12.2 ^b	145±27 ^a
Phosphatidylethanolamine	49.9±9.51 ^b	54.7±9.57 ^{ab}	69.3±12.9 ^a	70.5±14.1 ^a	68.9±17.5 ^a	54.5±8.15 ^a	73.4±9.82 ^a
Phosphatidylserine/phosphatidylinositol	53.1±16.7 ^b	69±20 ^{ab}	89.6±15.2 ^a	89.7±25.7 ^a	95.1±22.3 ^a	69.1±12.9 ^a	92.9±16.5 ^a
Phosphatidylcholine	77.3±19.2 ^b	81.1±13.6 ^{ab}	115±20.3 ^a	103±19.4 ^a	116±15.3 ^a	72.6±7.72 ^b	121±16.5 ^a
Lysophosphatidylcholine	11.7±11.2 ^a	3.12±5.7 ^a	6.05±10.5 ^a	19.3±14.5 ^a	13.5±14.8 ^a	15.1±12 ^a	6.1±9.15 ^a
ΣStorage	66.6±6.91 ^a	64.3±6.5 ^a	49.8±7.85 ^b	54.3±8.23 ^a	50.2±5.65 ^a	63.6±6.05 ^a	48.8±7.05 ^a
ΣStructural	33.4±6.91 ^b	35.7±6.5 ^b	50.2±7.85 ^a	45.7±8.23 ^a	49.8±5.65 ^a	36.4±6.05 ^a	51.2±7.05 ^a
Storage:Structural	2.34±0.66 ^a	2.1±0.64 ^{ab}	1.17±0.45 ^b	1.55±0.59 ^a	1.14±0.33 ^a	1.99±0.42 ^a	1.09±0.29 ^a

7

Table 2 (on next page)

Fatty acid and fatty alcohol composition (mg g lipid⁻¹) of distal intracolony locations in two size classes of *Acropora millepora* colonies.

L-centre: large colony centre, L-33: 33.3% of the longitudinal radius length, L-66: 66.6% of the longitudinal radius length, L-edge: large colony edge, S-centre: small colony centre, S-50: 50% of the longitudinal radius length, S-edge: small colony edge (S-edge). Values are presented as means \pm SEM. For each colony size, values in the same row size that do not share the same superscripts are significantly different ($P < 0.05$).

1 *Table 2*

2 Fatty acid and fatty alcohol composition (mg g lipid⁻¹) of distal intracolony locations in two size classes of *Acropora millepora*
3 colonies. L-centre: large colony centre, L-33: 33.3% of the longitudinal radius length, L-66: 66.6% of the longitudinal radius length,
4 L-edge: large colony edge, S-centre: small colony centre, S-50: 50% of the longitudinal radius length, S-edge: small colony edge (S-
5 edge). Values are presented as means ± SEM. For each colony size, values in the same row size that do not share the same superscripts
6 are significantly different ($P < 0.05$).

Fatty Acids (mg g lipid ⁻¹)	Small			Large			
	Centre	S-50	Edge	Centre	L-33	L-66	Edge
14:0	25.2±4.32 ^a	21.9±2.71 ^a	14.4±3.14 ^b	21.2±3.95 ^{ab}	17.8±2.97 ^{ab}	25.8±3.97 ^a	14.9±2.52 ^b
16:0	224±38.6 ^a	192±22 ^{ab}	134±29.4 ^b	188±32.2 ^{ab}	159±23.4 ^b	238±32.4 ^a	144±26.2 ^b
18:0	38.1±6.19 ^a	33.6±4.22 ^a	33.5±3.88 ^a	30.8±3.11 ^a	29.4±3.64 ^a	33.6±3.66 ^a	33.1±3.76 ^a
ΣSFA	296±48.9 ^a	255±28 ^{ab}	189±35.9 ^b	248±37.5 ^{ab}	214±28.2 ^b	306±38.9 ^a	199±31.3 ^b
16:0-OH	68.4±13 ^a	59.8±9.22 ^a	37.7±9.63 ^b	55.1±11.7 ^{ab}	46.9±8.75 ^b	75.8±10.2 ^a	44±9.84 ^b
18:1n-9	18.4±3.41 ^a	16.4±2.42 ^a	11.1±2.72 ^b	19.5±3.76 ^{ab}	15.8±1.97 ^{ab}	24.4±3.71 ^a	14.2±2.93 ^b
20:1n-11	14.3±1.9 ^a	11.8±1.23 ^{ab}	9.53±1.36 ^b	12.8±1.48 ^a	11.8±1.37 ^a	14.6±1.74 ^a	11.1±1.2 ^a
ΣMUFA	51.2±6.99 ^a	44.5±4.44 ^{ab}	32.8±5.73 ^b	48.8±7.54 ^{ab}	41.9±4.75 ^b	59.4±7.49 ^a	38.7±5.7 ^b
18:3n-6	24.8±4.38 ^a	21.2±2.34 ^a	13.4±3.18 ^b	20.1±3.87 ^{ab}	17±2.3 ^b	26.6±3.48 ^a	15.7±3.28 ^b
20:4n-6	8.22±1.4 ^b	8.3±1.63 ^{ab}	11.2±1.26 ^a	8.39±1.6 ^b	8.79±1.34 ^b	8.13±0.81 ^b	12.5±1.64 ^a
20:5n-3	21.4±1.85 ^a	19.6±2.72 ^a	21.7±2.76 ^a	19.1±1.5 ^a	19.7±2.15 ^a	20.9±1.93 ^a	23.4±2.1 ^a
22:6n-3	16.9±3.02 ^a	14.5±2.08 ^{ab}	11.1±2.29 ^b	13.6±2.4 ^a	11.9±1.88 ^a	17±2.47 ^a	12.3±1.81 ^a
ΣPUFA	164±21 ^a	146±15.9 ^{ab}	119±17.6 ^b	142±16.5 ^{ab}	128±14 ^b	175±19.5 ^a	136±16.2 ^b
ΣFatty alcohol	75.4±13.3 ^a	66.5±9.66 ^{ab}	44.6±10.2 ^b	61.4±11.9 ^b	53.1±8.79 ^b	82.9±10.8 ^a	51.7±10.1 ^b
Total	519±75.1 ^a	452±46.8 ^{ab}	347±58.6 ^b	445±61.3 ^{ab}	391±46.1 ^b	547±66 ^a	382±52.6 ^b
Σn-3 PUFA	44.9±4.65 ^a	40.2±5.04 ^a	39.3±5.16 ^a	38.8±3.31 ^a	37.8±4.04 ^a	44.5±4.94 ^a	43.1±3.93 ^a

7

Σn-6 PUFA	26.2±2.27 ^a	24.9±3.38 ^a	28.1±2.53 ^a	28.2±3.27 ^a	26.5±3.1 ^a	27.7±2.36 ^a	33.1±3.06 ^a
------------------	------------------------	------------------------	------------------------	------------------------	-----------------------	------------------------	------------------------

Table 3 (on next page)

Fatty acid and fatty alcohol composition (% fatty acids) of distal intracolony locations in two size classes of *Acropora millepora* colonies.

L-centre: large colony centre, L-33: 33.3% of the longitudinal radius length, L-66: 66.6% of the longitudinal radius length, L-edge: large colony edge, S-centre: small colony centre, S-50: 50% of the longitudinal radius length, S-edge: small colony edge (S-edge). Values are presented as means \pm SEM. For each colony size, values in the same row size that do not share the same superscripts are significantly different ($P < 0.05$).

1 *Table 3*

2 Fatty acid and fatty alcohol composition (% fatty acids) of distal intracolony locations in two size classes of *Acropora millepora*
3 colonies. L-centre: large colony centre, L-33: 33.3% of the longitudinal radius length, L-66: 66.6% of the longitudinal radius length,
4 L-edge: large colony edge, S-centre: small colony centre, S-50: 50% of the longitudinal radius length, S-edge: small colony edge (S-
5 edge). Values are presented as means \pm SEM. For each colony size, values in the same row size that do not share the same superscripts
6 are significantly different ($P < 0.05$).

Fatty Acids (% fatty acids)	Small			Large			
	Centre	S-50	Edge	Centre	L-33	L-66	Edge
14:0	4.8 \pm 0.16 ^a	4.83 \pm 0.22 ^a	4.05 \pm 0.29 ^b	4.66 \pm 0.29 ^a	4.49 \pm 0.31 ^a	4.67 \pm 0.26 ^a	3.83 \pm 0.21 ^b
16:0	42.6 \pm 1.68 ^a	42.3 \pm 1.74 ^a	37.5 \pm 2.69 ^b	41.4 \pm 1.68 ^a	40.4 \pm 1.46 ^{ab}	43.2 \pm 0.85 ^a	36.8 \pm 2.2 ^b
18:0	7.43 \pm 0.85 ^b	7.45 \pm 0.63 ^b	10 \pm 1.05 ^a	7.27 \pm 0.92 ^{ab}	7.66 \pm 0.77 ^{ab}	6.23 \pm 0.56 ^b	8.92 \pm 0.8 ^a
ΣSFA	56.6 \pm 1.39 ^a	56.3 \pm 1.52 ^a	53.8 \pm 1.79 ^a	55.2 \pm 1.17 ^a	54.6 \pm 1.13 ^{ab}	55.6 \pm 0.79 ^a	51.6 \pm 1.74 ^b
16:0-OH	13 \pm 0.76 ^a	13.1 \pm 0.88 ^a	10.4 \pm 1.13 ^b	12 \pm 1.12 ^{ab}	11.8 \pm 1.11 ^{ab}	13.8 \pm 0.5 ^a	11.1 \pm 1.18 ^b
18:1n-9	3.59 \pm 0.62 ^a	3.67 \pm 0.47 ^a	3.17 \pm 0.51 ^a	4.27 \pm 0.36 ^a	4.09 \pm 0.35 ^a	4.41 \pm 0.27 ^a	3.7 \pm 0.41 ^a
20:1n-11	2.77 \pm 0.17 ^a	2.63 \pm 0.23 ^a	2.81 \pm 0.23 ^a	2.93 \pm 0.25 ^a	3.07 \pm 0.26 ^a	2.7 \pm 0.18 ^a	2.99 \pm 0.25 ^a
ΣMUFA	9.97 \pm 0.95 ^a	9.92 \pm 0.68 ^a	9.49 \pm 0.71 ^a	10.9 \pm 0.35 ^a	10.8 \pm 0.4 ^a	10.8 \pm 0.23 ^a	10.1 \pm 0.4 ^a
18:3n-6	4.31 \pm 0.68 ^a	4.39 \pm 0.61 ^a	6.59 \pm 1.14 ^b	4.57 \pm 0.64 ^{ab}	5.18 \pm 0.62 ^a	3.91 \pm 0.33 ^{ab}	6.47 \pm 0.87 ^b
20:4n-6	3.23 \pm 0.24 ^b	3.17 \pm 0.26 ^b	3.14 \pm 0.16 ^a	3.01 \pm 0.2 ^b	2.99 \pm 0.2 ^{ab}	3.08 \pm 0.13 ^b	3.23 \pm 0.2 ^a
20:5n-3	4.73 \pm 0.44 ^b	4.72 \pm 0.31 ^b	3.76 \pm 0.43 ^a	4.4 \pm 0.32 ^b	4.32 \pm 0.16 ^{ab}	4.85 \pm 0.2 ^b	4.01 \pm 0.36 ^a
22:6n-3	1.76 \pm 0.55 ^a	1.88 \pm 0.44 ^a	3.52 \pm 0.76 ^a	2.13 \pm 0.59 ^a	2.37 \pm 0.45 ^a	1.55 \pm 0.23 ^a	3.54 \pm 0.7 ^a
ΣPUFA	19 \pm 1.67 ^b	19.2 \pm 1.52 ^b	24.2 \pm 2.54 ^a	20.5 \pm 1.84 ^b	21.2 \pm 1.72 ^{ab}	18.3 \pm 0.77 ^b	25 \pm 2.36 ^a
ΣFatty alcohol	14.4 \pm 0.62 ^a	14.5 \pm 0.78 ^a	12.5 \pm 0.91 ^b	13.4 \pm 1.01 ^a	13.4 \pm 0.98 ^a	15.1 \pm 0.49 ^a	13.2 \pm 0.95 ^a
Total (% lipid)	51.9 \pm 7.5 ^a	45.2 \pm 4.7 ^a	34.7 \pm 5.9 ^b	44.5 \pm 6.1 ^{ab}	39.1 \pm 4.6 ^b	54.7 \pm 6.6 ^a	38.2 \pm 5.2 ^b

Σ n-3 PUFA	8.87±0.86 ^b	8.92±0.91 ^b	11.7±1.43 ^a	9.03±0.74 ^b	9.81±0.8 ^{ab}	8.21±0.42 ^b	11.7±1.26 ^a
Σ n-6 PUFA	5.39±1.07 ^b	5.57±0.84 ^b	8.67±1.46 ^a	7±1.47 ^{ab}	7.04±1.02 ^{ab}	5.2±0.48 ^b	9.21±1.4 ^a

7